Wave energy conversion by multi-mode exciting wave energy converters arrayed around a floating platform

Yong Cheng[a], Weifeng Liu[a], Saishuai Dai[b,*1], Zhiming Yuan[a, b], Atilla Incecik[b]

[a]*School of naval architecture and ocean engineering, Jiangsu University of Science and Technology, Zhenjiang, 212003, China*

[b]*Naval Architecture, Ocean and Marine Engineering Department, University of Strathclyde, Glasgow, United Kingdom*

Abstract

An array of compact, portable and stable Wave Energy Converters (WECs) integrated with an offshore floating platform can reduce the platform's motion response to waves, and extract wave energy simultaneously through multiple Power Take-Off (PTO) units. This paper proposes an innovative hybrid system composed of a cylindrical free-floating platform and four point-absorber type WECs hinged at the external structure of the cylindrical platform. The relative motions between a WEC and the platform drive a PTO-system, and thus desirable wave energy conversion is achieved from combining multiple WECs with multi-mode motions constructively. To confirm feasibility and hydrodynamics performance of the proposed concept, multi-body computational models for different scenarios are developed. The wave focusing toward WECs are realized by the array reflection, while the presence of near-trapping waves amplifies energy dissipation. The seaward and leeward WECs are more sensitive on the array interval than those lateral WECs. Additionally, shallower and deeper submergences are preferred for WECs, respectively, resulting into multi-body resonances across a broadband wave period. For the discrete PTO system, different optimized damping coefficients are recommended to guarantee the high energy absorption regardless of wave periods. The present WEC-platform system can harvest wave energy in an omnidirectional manner.

Keywords

Wave energy converter, Floating platform, Multi-mode motion, Conversion efficiency, Array layout

List of abbreviations：

Nomenclature

Symbols		*Abbreviations*	
b_{pto}	Energy extraction damping [Nms/rad]	AG	Anti-pitching Generating
D	Diameter of the platform [m]	CFD	Computation Fluid Dynamics
d	Diameter of the WEC [m]	D-HRWEC	Designed Hinged Raft Wave Energy Converter
d_1	Draft of the platform [m]		
d_2	Draft of the WEC [m]	M-WEC	Multi-mode Wave Energy Converter
d_g	Gap distance [m]		
H_i	Incident wave height [m]	MEWEC	Multi-mode Exciting Wave Energy

*Corresponding author: Saishuai Dai, mainly research in hydrodynamic performance of wave energy converters
E-mail: saishuai.dai@strath.ac.uk

h	Water depth [m]		Converter
L_1	Height of the central hinge from the water surface [m]	OB	Oscillating Buoy
		OWSC	Oscillating Wave Surge Converter
L_2	The length from two ends of the hydraulic piston cylinder to the central hinge point [m]	PTO	Power Take Off
		RANS	Reynolds-Averaged Navier-Stokes
η_s	Energy conversion efficiency of the seaward WEC	SD	Salter's Duck
		VLFS	Very Large Floating Structure
η_b	Energy conversion efficiency of the backward WEC	VOF	Volume of Fluid
		WEC	Wave Energy Converter
η_l	Energy conversion efficiency of the lateral WEC		
η_o	Energy conversion efficiency of the overall system		
λ	Wavelength		
c	Damping coefficient of PTO		

1 Introduction

Substitute traditional oil, coal and natural gas with renewable and sustainable energy can significantly accelerate the process of achieving the net-zero greenhouse gas emissions target by 2050 [1], which is consistent with efforts to limit the long-term rising global average temperature by 1.5º [2]. Ocean energy exploitations [3], as a technically feasible, cost-effective and socially acceptable pathway of the clean energy transition, are gradually drawing wider attention [4], especially for the sustainable energy supply for isolated islands or coastal communities. Nonetheless, for wave energy systems, the industrialization progress needs to be consolidated [5], in terms of reliability, longevity, affordability and maintainability [6]. Many researchers and engineers deepen their efforts to evaluate the pertinence of wave energy harvesting capacity [7] which is the one of most prominent hurdles [8]. It is the motivation of this paper to end up with solutions that are practical, affordable and with an exemplary hydrodynamic efficiency analysis.

Generally, when waves propagate toward nearshore zones, only approximately 30% of wave energy can be retained due to wave refraction, breaking and sea-bed friction [9], and most of wave energy is concentrated at offshore zones. Deploying geometrically simple Wave Energy Converters (WECs) near a floating offshore platform could provide daily power need of onboard equipment and sensors. Besides, such a configuration can also promote more efficient ocean space utilization and create synergies between the offshore platform and the WEC, e.g. sharing mooring systems [10]. Dan et al. [11] investigated the motion characteristics of an Anti-pitching Generating Wave Energy Converter (AGWEC) and a floating platform in waves using the Computational Fluid Dynamics (CFD) method and viscosity-corrected potential flow theory. By comparing the computational results of the CFD method using Star CCM+ with the viscous modified potential flow theory method, the versatility of the two methods was confirmed. Additionally, Zhang et al. [12] developed a WEC that uses a hydraulic PTO mechanism. In order to capture wave energy and prevent the platform from tilting, this WEC device is used in conjunction with a modular floating platform. Zhang et al. [13] proposed an integrated WEC to be installed on a very large floating platform consisting of several modular semi-submersible type units. By placing the PTO system in the gap between each semi-submersible platform module, this integrated system effectively reduces the platform's pitching motion and offers a high power capture coefficient. Moreover, Nguyen et al. [14] proposed

Journal Pre-proof

the use of modular raft WEC on the leading edge of a rectangular Very Large Floating Structure (VLFS) to mitigate the hydrodynamic response of the VLFS under wave excitation and extract wave energy. This modular design makes installation easier and more flexible for adapting to different forms. Following the same approach, Nguyen et al. [15] introduced an Oscillating Wave Surge Converter (OWSC)-type device, which includes an underwater vertical flap connected to the front of a floating platform using a hinge and a PTO system. The device's power capture factor is high for most wave periods, and the OWSC is more effective at reducing the platform's hydrodynamic response than fixed underwater vertical damping flaps [16]. Zhang et al. [17] suggested placing a PTO system between the runway of a floating flexible runway and the supporting floating columns. This mechanism can convert a portion of the flexible runway's vertical deformation into useful energy and minimize the overall vertical displacement. Zhou et al. [18] looked into a hybrid system consisting of a floating wind turbine and an array of WECs. Power extraction enhancement was observed in their design whenever the floating wind turbine and the WECs are in synchronous mode, irrespective of the detailed configuration of the WEC array

A practical challenge of improving the energy conversion efficiency of WECs is related to harvesting modes. For example, the theoretical maximum power capture width of a point-absorber type WEC is $\lambda/2\pi$ for heave only motion, where λ is the wavelength. On the other hand, for surge or pitch type WEC, the theoretical maximum capture width is doubled. The theoretical maximum capture width can even be tripled if both heave and surge/pitch is used for power generation [19], indicating the superiority of multi-mode extraction WECs over single-mode ones in terms of theoretical potential. Ma et al. [20] investigated the wave energy conversion and the period of amplitude variation of a multi-degrees-of-freedom Oscillating Buoy (OB) type WEC. Their findings suggest that the periodic variation in the amplitude of floater motion is primarily caused by the surge motion. The elastic and damping coefficients' contributions to energy conversion efficiency are influenced by the wave height. In addition, in contrast to most raft devices and point absorbers, Liao et al. [19] suggested a multi-float Multi-mode Wave Energy Converter (M-WEC), which provides a number of degrees of freedom for power extraction. A self-contained, comprehensive, non-causal optimum control system that can precisely forecast the excitation force of incident waves has been devised to further enhance the power extraction performance. P. Stansby et al. [21] proposed a three-float broadband resonant line absorber which included the surge response for wave energy conversion. A 1:8 scaled experimental results indicate the importance of surge force and heave resonance in terms of drag reduction and widening the capture width. Based on this investigation, Stansby et al. [22] optimized the power capture of the three-float line absorber WEC M4 through experiments and linear diffraction modelling. It was discovered that when a separation between the front two floats is at least 1.5 times longer than that of the back two floats can lead to better power capture performance. After that, D.R. Lande-Sudall et al. [23] laid the foundation of a numerical methodology which integrates hydrodynamic forces into a moving frame. The method was applied to simulate a 3 floats, a 6 floats and a 8 floats WECs, respectively, in both regular and irregular wave conditions. Results were successfully validated against both the vector method and experimental measurements. This approach offers a more natural and versatile solution for complex multi-body, multi-hinge fluid dynamics systems. As an extension, Tran et al. [24] proposed a design strategy in which the surge, heave, and pitch degrees of freedom were decoupled and were designed to have to different natural frequencies. This configuration can significantly enhance the absorbed power of multi-mode WEC, especially in terms of capture bandwidth.

In order to accurately assess the total energy conversion of WEC arries, three-dimensional interaction between each WEC should be taken into consideration, particularly when the spacing between each WEC in the array is comparable with the incident wavelength. Zeng et al. [25] proposed a WEC with five degrees of freedom and studied the power generation capacity of a single WEC, a two-WEC array, and a five-WEC array. The results show that the fixed array layout is advantageous for suppressing power output fluctuation. Through numerical simulations, Fuat Kara [26] examined the impact of separation distance between WECs in array systems and wave heading angle on energy absorption, where the WEC extracts energy in both sway and heave mode. Numerical simulation indicates that the sway mode has a broader energy absorption bandwidth compared to the heave mode. Wave interactions are stronger when WECs in the array system are in close proximity, and as separation between WECs increases, these wave interactions decrease significantly. Yazdi et al. [27] proposed a new wave energy device, which comprises a floating semi-submersible platform and a set of Salter's duck (SD) WECs. The performance of the integrated system was then studied with varying numbers of WECs under different wave periods and wave heights. He et al. [28] examined the performance of a trussed octagonal platform coupled with multiple WECs and investigated the multibody hydrodynamic interaction between the platform and WECs. Numerical results indicate that multi-body interactions have a significant effect on power absorption. Afterward, He et al. [29] examined the impact of platform motion on power absorption of a circular array of WECs. They discovered that the heave motion of the platform enhanced the power absorption of the WEC array for most tested wave frequencies, whereas the pitch motion of the platform had the opposite effect. Kamarlouei et al. [30] found that positioning arrayed WECs around a floating platform can generate restoring moments for the platform and thus contribute to pitch motion control. Furthermore, a preliminary experiment [31] was conducted on concentrically arranged WECs connected to a floating offshore platform. The experiment revealed that the reduction of the heave and pitch motion of the platform depends on the equivalent damping introduced by the power generation of the WECs. Zhao et al. [10] developed a frequency-domain model based on multi-body dynamics and beam bending theory to analyze the hydroelasticity and coupling dynamics of a floating platform in waves, as well as the wave power extraction performance. They found that neglecting hydroelasticity at a specific frequency leads to an overestimation of the hydrodynamic efficiency of the buoy array.

Although the interference effects of WECs-platform integrated systems are crucial, most of the existing works mainly focused on a single model wave energy harvesting manner, i.e. heave motion of WECs installed on a fixed platform. The effect of the proximity between WECs in such a WECs-platform is not well understood, particularly when multiple degrees-of-freedom of WECs are used for energy production. In this paper, an array of point-absorber type WECs hinged to a cylindrical offshore platform is considered. Each in the array WEC is connected to the floating platform through a PTO unit, and the Power generation is driven by the relative motion between the WEC and the floating platform. The current study aims to complement and address some fundamental questions though numerical simulations, i.e. How do the in-phase and out-of-phase motions between WECs and the platform affect wave energy extraction? Would it be possible to enhance the power generation by arrange the WECs in an optimized configuration?

This paper is arranged as follows. Section 2 presents the development of a multi-body hydrodynamic model based on the nonlinear mode expansion method in time domain. The numerical results with convergence analysis are compared with published experimental results in

Section 3. Section 4 discusses the nonlinear numerical results. Finally, conclusions are drawn in Section 5.

2 Numerical model

In this research, the Eulerian multiphase flow model employs the incompressible Reynolds-Averaged Navier-Stokes (RANS) equations for water-air mixtures, using the Volume of Fluid (VoF) method to track interface motion between the air and water phases. In this section, a three-dimensional numerical wave tank and hybrid system were built by using Star CCM+ software to investigate the interaction of the wave with hybrid systems.

2.1 Governing equation

Fluid in nature can be governed by mass conservation and momentum conservation law. Equation (1) gives the mass conservation equation (also known as continuity equation),

$$\frac{\partial \rho}{\partial t} + \nabla \cdot (\rho \boldsymbol{u}) = 0 \tag{1}$$

where ρ refers to the fluid density, t refers to the time, $\nabla = (\partial / \partial x, \partial / \partial y, \partial / \partial z)$ is the differential operator. For incompressible fluids ρ is constant, and the above formula can be simplifed as:

$$\nabla \cdot \boldsymbol{u} = 0 \tag{2}$$

The momentum conservation equation can be expressed as:

$$\frac{\partial (\rho \boldsymbol{v})}{\partial t} + \nabla \cdot \left(\rho \boldsymbol{v} \cdot \boldsymbol{v}^{\mathrm{T}} \right) = \nabla \cdot \boldsymbol{\sigma} + \boldsymbol{f}_b \tag{3}$$

where $\boldsymbol{f}_b$ refers to the resultant force of various volume forces acting on the unit volume of the continuum, $\boldsymbol{\sigma}$ refers to the stress tensor. For fluids, the stress tensor is usually written as the sum of normal stress and shear stress, so $\boldsymbol{\sigma} = -p\boldsymbol{I} + \boldsymbol{T}$. Among them, p is the pressure, $\boldsymbol{T}$ refers to the viscous stress tensor, and we get:

$$\frac{\partial (\rho \boldsymbol{v})}{\partial t} + \nabla \cdot \left(\rho \boldsymbol{v} \cdot \boldsymbol{v}^{\mathrm{T}} \right) = -\nabla \cdot (p\boldsymbol{I}) + \nabla \cdot \boldsymbol{T} + \boldsymbol{f}_b \tag{4}$$

The total mass conservation equation for all phases is given by:

$$\frac{\partial}{\partial t} \left(\int_V \rho dV \right) + \oint_A \rho \boldsymbol{v} \cdot d\boldsymbol{a} = \int_V S dV \tag{5}$$

where $\boldsymbol{a}$ refers to the surface area vector, $\boldsymbol{v}$ is the mixture (mass-averaged) velocity, S is a mass source term that is related to the phase source term as follows:

$$S = \sum_i S_{a_i} \cdot \rho_i \tag{6}$$

The VOF wave model is used to simulate surface gravity waves at the interface between air and water. Fifth order Stokes wave theory was adopted for wave generation in the current simulation to account for wave non-linearity. This wave is closer to a true wave than a wave generated by first-order methods. Wave shape and wave phase speed depend on water depth, wave height and current. The Ursell number U_R is defined as:

$$U_R = \frac{H\lambda^2}{d^3} \tag{7}$$

where H is the wave height, λ is the wavelength, and d is the water depth.

2.2 WEC-platform integrated system and numerical PTO model

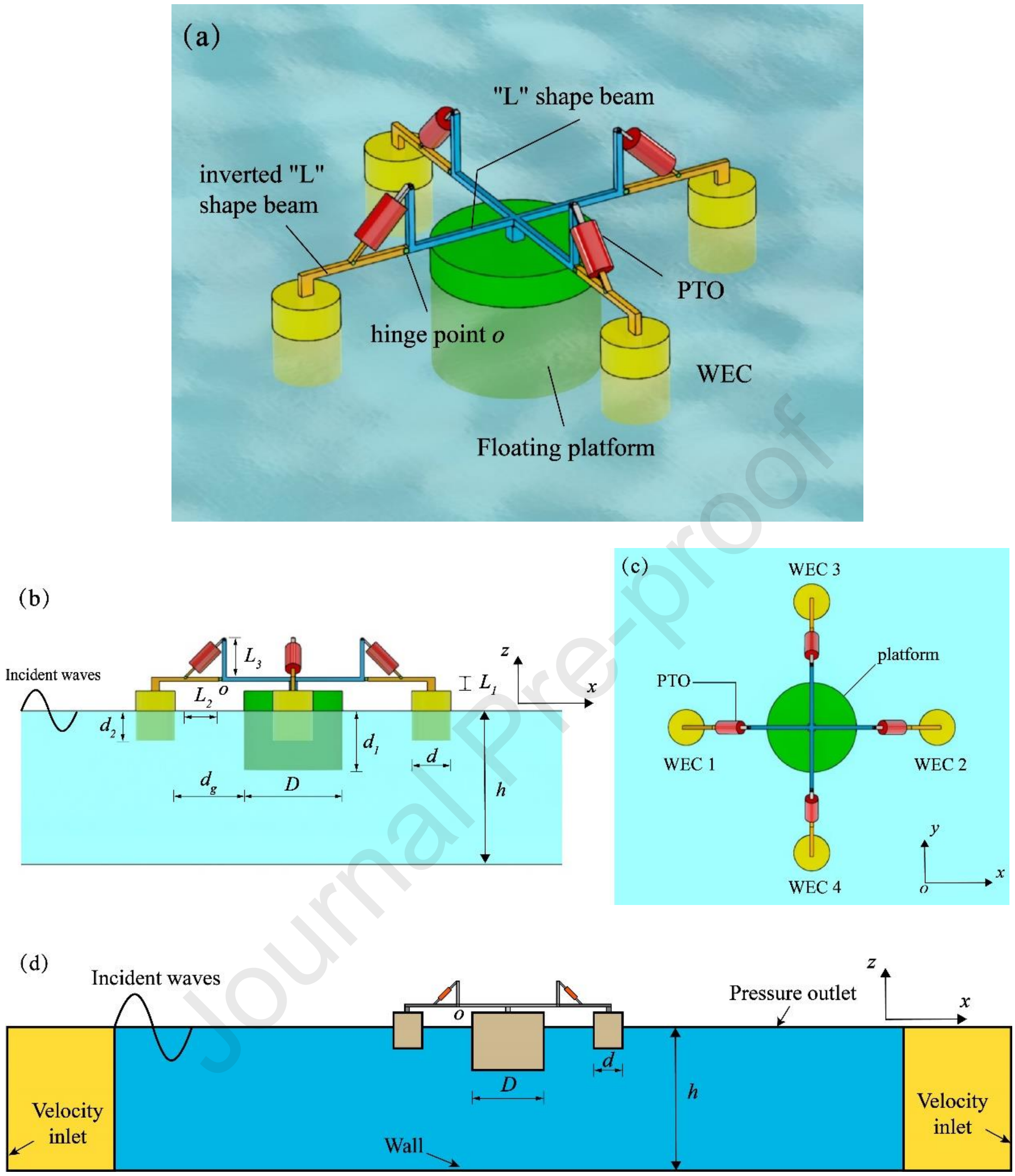

Fig. 1. A diagram of MEWEC in a 3-D wave tank: (a) bird's-eye view (b) Side view (c) Top view (d) simulation domain

As mentioned previously, the maximum theoretical capture width of a multi-degree freedom WEC is much higher than that of a heave only type WEC. The current study therefore proposes a Multi-mode Exciting WEC (MEWEC) as illustrated by **Fig. 1**, where 4 WECs are symmetrically deployed around a central cylindrical floating platform and are connected through articulated mechanisms. The articulated mechanism consists of an "L" shape beam fixed to the platform, and an inverted 'L' shape beam rigidly connected to a WEC (**Fig. 1**(a)). The two beams are then connected together through a central hinge denoted as shown in **Fig. 1**. Between the two beams, a Hydraulic PTO system is installed, with one end hinged to the L beam and the other hinged to the inverted L beam. When subject to waves, the relative motion between the WEC and the platform forces the two beams to rotate about the central hinge point o and drives the hydraulic PTO system, power can thus be generated. It should be noted that in addition to heave responses of the WEC and the platform, any other degrees-of-freedom motion response that will cause relative rotation between the two beams will contribute to energy production, e.g. pitch motion of the platform.

Key geometry dimensions of the hybrid system include: the diameter of the platform D, the diameter of the floater d, the draft of the platform d_1, the draft of the floaters d_2, the gap distance between the platform and the WEC d_g. the height of the central hinge from the water surface L_1, the length from two ends of the hydraulic piston cylinder to the central hinge point o L_2 and L_3. The distance between the central hinge point and the center of the platform is equal to the distance between the central hinge point and the WEC.

The simulation domain is illustrated by **Fig. 1** (d), with coordinate system indicated in both figures. In the simulations, wave propagates along the positive x-axis direction, pitch motion is defined as rotation about the y-axis, and the heave response is along the z-axis. The length of the computational domain in the x direction is approximately equal to 6 wavelengths, and the width is slightly larger than the sway response of the hybrid system in the y direction, which is approximately 5 times the diameter of the platform. The array is placed in the center of the flow field. In order to analyze the interaction between waves and floating bodies, overlapping grids were established on the outside of the platform and the four WECs. The left and right boundaries of the computational domain are defined as velocity inlets, top boundary of the domain is defined a pressure outlet, bottom boundary of the domain and the floater surface boundaries are both defined as non-slip walls. Lateral boundaries of the simulation domain in the y direction are defined as symmetry boundaries. The hybrid system may drift with the incident wave because the mooring system of the device is not considered in this paper. With this in mind, the x-direction freedom of the central floating platform is locked so that the device does not drift with the incident wave and the motion response will be more stable.

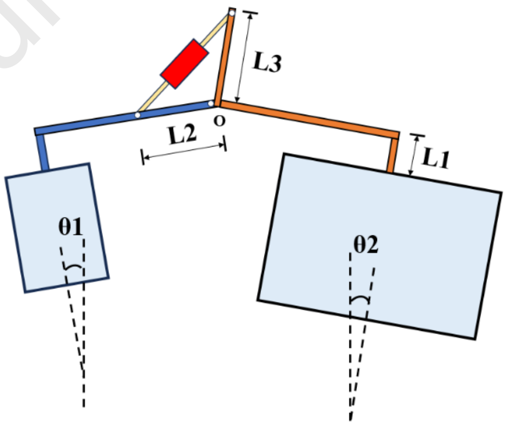

Fig. 2. A diagram of the articulated mechanism with hydraulic energy storage PTO system

The mechanical coupling between the WEC, the platform and the PTO system is achieved through a Dynamics Fluid Body Interaction (DFBI) model and mechanical joint module built in the software (see Star CCM+ user manual for details). Where the PTO system is simplified by imposing external damping moments onto the WEC and the platform respectively. The magnitude of the PTO damping moment [11] can be calculated by:

$$M_{PTO} = \pm \frac{\sqrt{2}}{2} c L_2^{\,2} \left(\dot{\theta}_1 - \dot{\theta}_2 \right) \tag{7}$$

where, the damping coefficient c of PTO is set as 300 (N/(m/s)), the length from the two ends of the hydraulic piston cylinder to the central hinge point is L_2=0.1m, $b_{pto} = \sqrt{2}cL_2^{\ 2}/2$, $\dot{\theta}_1$ and $\dot{\theta}_2$ refers to angular velocity of the platform and the floater which is determined by θ_1, θ_2 (rotation angles of the floating body and the floating platform as indicated by **Fig. 2**).

2.3 Wave energy capture factor

Capture factor is an important indicator equivalent to efficiency for WEC power capture performance evaluation, which is defined as the ratio between the captured power E_p to the wave power available to the WEC E_w.

The captured power E_p can be calculated by:

$$E_p = \frac{1}{2} b_{pto} \omega^2 \Omega^2 \tag{8}$$

Where, b_{pto} is the PTO damping converted to a rotational damping, for the above PTO model, $b_{pto} = \sqrt{2}cL_2^{\ 2}/2$, ω is the relative rotation frequency, Ω refers to the amplitude of the relative pitch angle between the platform and the WEC.

The average energy flow rate E_w of a linear wave can be expressed as:

$$E_w = \frac{1}{16} \frac{\rho g H_i^{\ 2} \omega D_y}{k} \left(1 + \frac{2kh}{\sinh 2kh} \right) \tag{9}$$

Where, ρ refers to the water density, g denotes the acceleration of gravity, H_i refers to the incident wave height, h refers to the water depth, D_y refers to the longitudinal width of the wave energy device and k is the wave number.

The capture factor η can be calculated by:

$$\eta = \frac{E_p}{E_w} \tag{10}$$

3 Convergence study and validation

3.1 convergence study

Prior to assessing the performance of the proposed hybrid system, a convergence test of the numerical simulation is conducted, and the detailed model parameters are listed in **Table 1**. Hereinafter, the whole length and height of the numerical tank are adopted as 6 times incident wavelength and 2 times the water depth, respectively, where both tank ends are imposed by wave forcing damping zone with 1.5 times incident wavelength. The tank height is set as 2 times water depth. Three different grid schemes i.e. coarse, moderate and fine cells are examined with wave period T=1s, wave height H_i=0.08 m, where the time step is fixed as dt=T/1000. The dynamic grid region near the hybrid WEC-platform system is further refined by using a trimmed grid generation to accurately simulate the multi-floater and multi-mode motions. Thus the cells in the dynamic grid region is shrunk to 3 times than those in the stationary region. The information exchange of two regions is interpolated on the interface based on the overset grid distinction. **Fig. 3** presents the motion response series of respective devices for different grid schemes, i.e. the pitch of the seaward and leeward WECs, the roll of the lateral WEC and the heave of the central platform, where due to the symmetry of flow field and floaters, only the results of one lateral WEC are presented. The numerical simulation lasts for 10 wave periods T which make the simulation present steady-state results. The results indicate that the coarse grid scheme affect the numerical accuracy compared with the fine scheme, especially for the seaward WEC with the relative difference exceeding 7%. However, the moderate scheme can provide almost identical results in reasonable computational time, where the relative amplitude and phase differences is smaller than 5% compared with the fine scheme. Similarly, after conducting different temporal schemes i.e. dt=T/800, dt=T/1000 and dt=T/2000, dt=T/1000 and moderate grid scheme are applied in Section 4 unless particularly specified.

Table 1 Key parameters of the numerical model.

Parameters	Value
Diameter of the platform (D) [m]	0.5
Diameter of the floater (d) [m]	0.2
Draft of the platform (d_1) [m]	0.3
Draft of the floater (d_2) [m]	0.15
Gap distance (d_g) [m]	0.35
Height of the central hinge from the water surface (L_1) [m]	0.15
Water Depth (h) [m]	0.7
Damping coefficient of PTO (c) [N/(m/s)]	300
The length from the two ends of the hydraulic piston cylinder to the central hinge point (L_2, L_3) [m]	0.1
Duration of the CFD simulation	10T

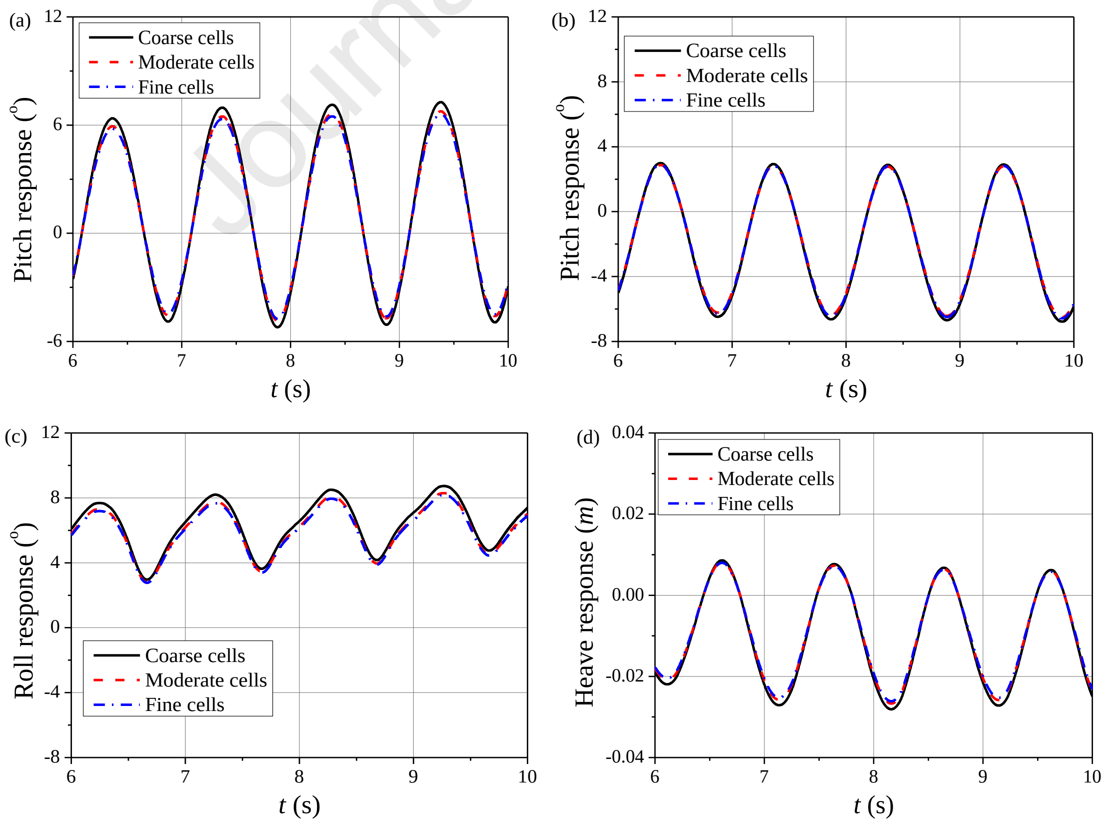

Fig. 3. Mesh convergence of moving responses i.e. (a) the pitch of seaward WEC, (b) the pitch of leeward WEC,

(c) the roll of lateral WEC and (d) the heave of central platform

3.2 Validation

A two-floater hinged raft WEC system , D-HRWEC, as shown in **Fig. 4**, is considered to validate the presented numerical model. This WEC system consists of two geometrically identical floater connected by a hinged arm combined with a controllable PTO unit which provides a linear rotational damping of b_{pto}=20 Nms/rad to the system. The numerical mesh for the simulation is shown in **Fig. 5**, where mesh refined are applied around the free surface and the floater to ensure accuracy. The corresponding experiments are conducted by Jin et al. [32]. **Fig. 6** presents a comparison of the relative pitch response between the numerical simulation and Jin's experiment results. As indicated, good agreement between the numerical simulation and the experiment are achieved. The slight over-prediction of numerical values at trough is probably due to the physical friction of the controllable PTO mounted inside the WEC device is not included in the numerical simulation.

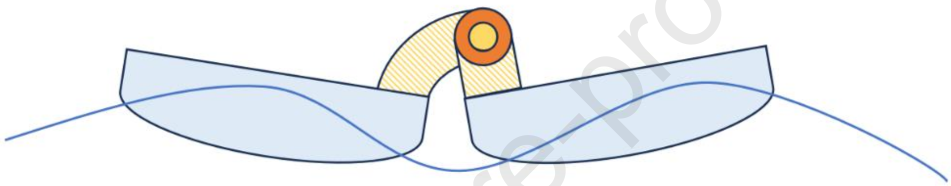

Fig. 4. Schematic of the D-HRWEC.

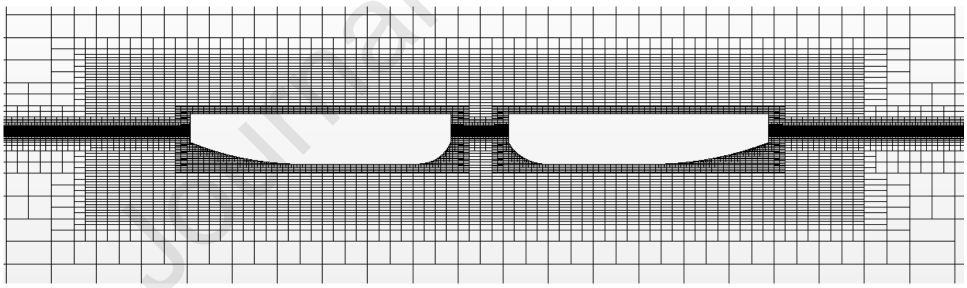

Fig. 5. Mesh generation for the validated model.

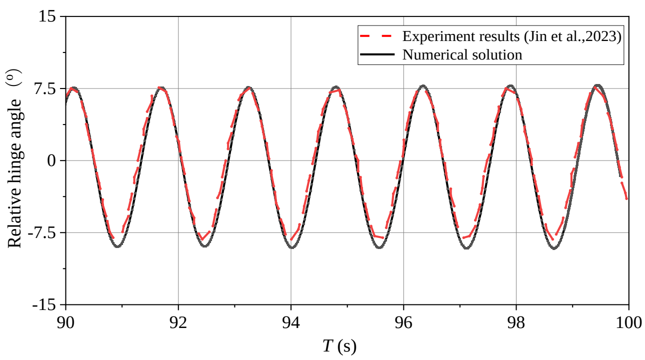

Fig. 6. Numerical and experimental comparison of relative hinge angles between floaters.

4 Numerical results

This section presents the numerical simulation results of the proposed hybrid system. The effect of the platform displacement on the capture factor of WECs is firstly examined, followed by an investigation of the near trap wave effect among multiple floating bodies. The effect of the draft of WECs, PTO and incident wave angles are also examined in this section. This paper selects the dimensionless period range of 2.4-6.4 because in this range MEWEC has better energy capture factor than other period range and it is easier to analyze the hydrodynamic performance of the device.

4.1 Coupling effect between WECs and the floating platform

The motions responses of the hybrid system are heavily dependent on the damping torque generated by the PTO unit, which, in turn, have a great impact on the radiated waves caused by the system's motion in waves. In addition, due to the relative larger size of the central cylindrical platform, diffraction is expected when subject to waves. Both those radiated and diffracted waves are dissipating energy and hence will lead to a lower power capture performance. On the other hand, due to the configuration of the current hybrid concept, it is possible that some of the radiated and diffracted waves generated by, say the front WEC, can be captured by other members in the system (i.e., the central platform and the other three WECs). To investigate the above, three different cylindrical diameters of the central platform are considered (the diameters are non-dimensionlized by the water depth here) i.e. D/h=0.4, 0.7 and 1.4, and other parameters are consistent with Table 1 in Section 3.1.

Fig. 7 presents the capture factor of the seaward WEC (η_s), the backward WEC (η_b), the lateral WEC (η_l) and the overall system (η_o) against dimensionless wave period $T(g/h)^{0.5}$. The values from **Fig. 7** (a) show that the maximum capture factor of the seaward WEC is enhanced when the diameter of the central platform increased, and the wave period at which the peak happens shifted from a lower to a higher wave period. Since waves transmit over a thinner platform more easily due to high penetrability and moves in phase with the hybrid system, a fatter platform directs to a constructive interaction and the out-of-phase motions between waves and the hybrid system are realized, causing the higher energy conversion. This illustrates a phase difference of motions between WECs and platform, thereby allowing it to harvest more long-period waves power. Inversely, a destructive effect on the wave energy conversion of the leeward WEC waves is observed, and the downside influence becomes stronger as the platform diameter increases, as presented in **Fig. 7** (b). This can be explained from the point of view of the shielding effect. The front platform provides a shielding area, and the WEC behind it receives less wave energy when the diameter of the platform increase. As shown in **Fig. 7** (c), the maximum capture factor of the lateral WEC placed nearby the cylindrical platform increases and shifts toward lower wave period for a fatter platform. What is more, when the platform diameter increases to D/h=1.4, apart from the maximum conversion at the WEC resonant period, there is a second peak capture factor (η_l =0.15) occurring at long-period waves, which is induced by the out-of-phase motions of waves and platform and contributes to the amplification of scattering waves.

It is remarkable that the double peak phenomenon would exist in the overall capture factor of the hybrid system, more significant i.e. η_t=0.23 and 0.26 when the platform diameter increasing to D/h=1.4. This is indicative of two-mode relative motions i.e. the lower period around $T(g/h)^{0.5}$=3.1 dominated by the heaving mode, the higher period around $T(g/h)^{0.5}$=4.7 controlled by the pitching or rolling mode. There is a sudden switch of η_t between these two natural periods, which is due to the fact that when the cylinders are closely adjacent, the near-trapping waves are generated in the array to divide waves into two parts i.e. small amount of scattering waves outward and near-standing waves with large amplitude oscillations of water surface. This near-standing resonance strengthens the wave energy dissipation. Consequently, the WECs cannot continuously harvest wave energy effectively in a wider range of $T(g/h)^{0.5}$.

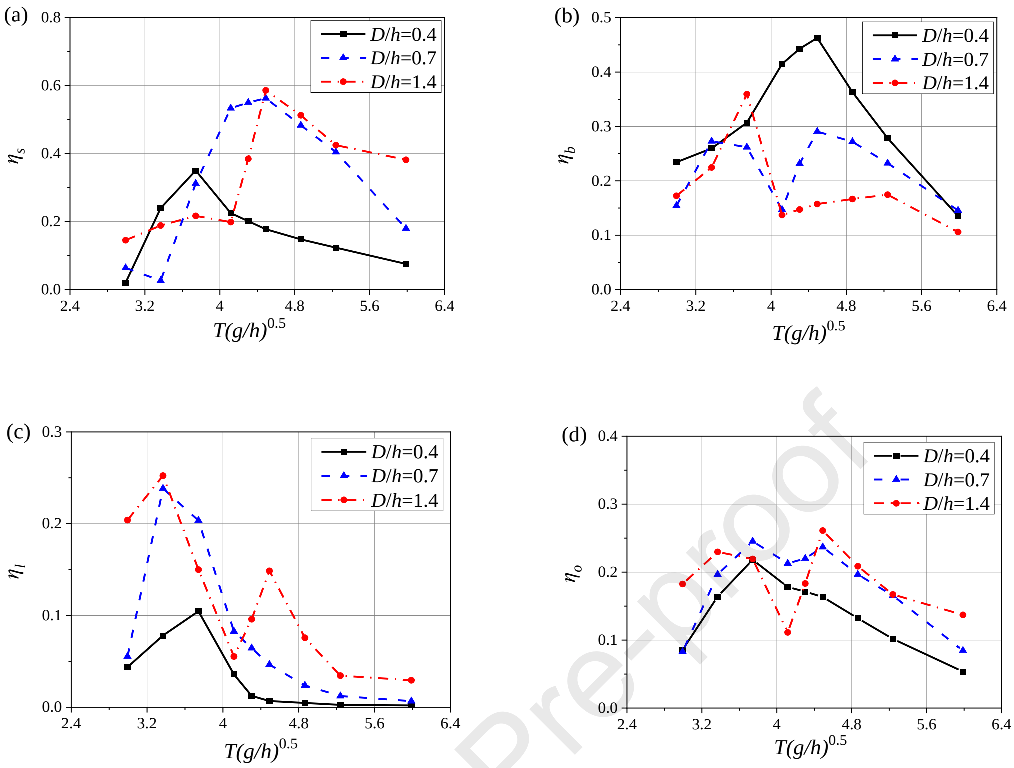

Fig. 7. Capture factor versus nondimensional wave period for different platform diameters.
(a) WEC1 (b) WEC2 (c) WEC3 and WEC4 (d) Overall hybrid system

4.2 Near-trapping wave effect among multiple floating bodies

In this paper, the geometries of WECs and platform are adopted as vertical cylinders, and thus the near-trapping waves would appear between the cylinders for certain wave periods and deliver a local water-surface oscillation dominated mainly by the piston-type mode. In these wave periods only a small amount of scattered wave energy is radiated outwards to the far field: the wave is trapped within the local vicinity of the cylinders, forming a near standing wave with much larger amplitude compared with that at other frequencies [33]. Therefore, the near-trapping wave effect on the energy conversion of the WEC-platform hybrid system are discussed in this section in more details. A series of dimensionless gap distances d_g/h between WECs and the platform are selected, and the efficiency contour of the overall system and respective devices is presented in **Fig. 8** (a)-(d).

It is remarkable from **Fig. 8** (a) that there are two same maximum capture factors i.e. η_s=0.63 over the calculated range of d_g/h and $T(g/h)^{0.5}$ for the seaward WEC, with one around d_g/h=0.36, $T(g/h)^{0.5}$=3.7, and another at d_g/h=0.68, $T(g/h)^{0.5}$=4.7. As gap distance increases, the conversion efficiency of the seaward WEC vanishes in short-period waves but first increases and then decays in long-period waves. This can be deduced from the relatively high ratio of the gap distance and the incident wavelength. It is conjectured that the WECs can be ultimately considered as isolated devices approximately in short-period waves when the gap distance increases. This would produce near-trapping waves in long-period waves, and further augment capture factor of WECs. Different near-trapping wave regions are generated as the gap distance increases. For the backward WEC, as presented in **Fig. 8** (b), there are two maximum values of η_s in the computed period range regardless of the gap distance. More specifically, the larger peak occurs around $T(g/h)^{0.5}$=3.5 but the smaller peak is at $T(g/h)^{0.5}$=5.0. In short-period waves, the backward-WEC performance is reinforced as the gap distance increases due to the mitigation of shielding effect provided the central platform. There is a period region 3.6<$T(g/h)^{0.5}$<4.2 of near-trapping waves, which is dependent of gap distance. The lateral WEC works nearly in short-period waves, although the magnitude of the maximum value is merely η_s=0.24, as presented in **Fig. 8** (c). This is because s the lateral WECs are inline with the platform, it moves almost in phase with the platform in long waves, resulting little relative motion between the two and hence little power can be captured.

As a comparison, the overall capture factor as presented in **Fig. 8** (d), are found to reach the maximum value 0.31 at the minimum gap distance d_g/h=0.36. Actually, the gap distance less than d_g/h=0.9 would be a good choice for the favorable performance of WECs over a broadband (3.1<$T(g/h)^{0.5}$<5.5). These results illustrate that a floater is subjected to a pulse velocity in one mode, which will in turn produce the same mode force on the adjacent floater after a finite time t equal to waves propagating inside the gap between the two floaters, where scattering wave energy is blocked. This means that energy is trapped in the gap between the floating bodies. And when a wave reflects off the floating bodies, only a small portion of the energy is radiated outward. Therefore, the larger gap distance means the weaker multi-body interaction, weakening the multi-mode relative motions of WECs and platform. As the gap distance d_g/h continues to increase, two higher energy conversion areas can be found, which is because long-period waves transmit inside the gap more easily and are focused to strengthen water column oscillation. However, energy conversion is suppressed at the region between the two high regions, generating a 'V' shape area of η_o>0.13.

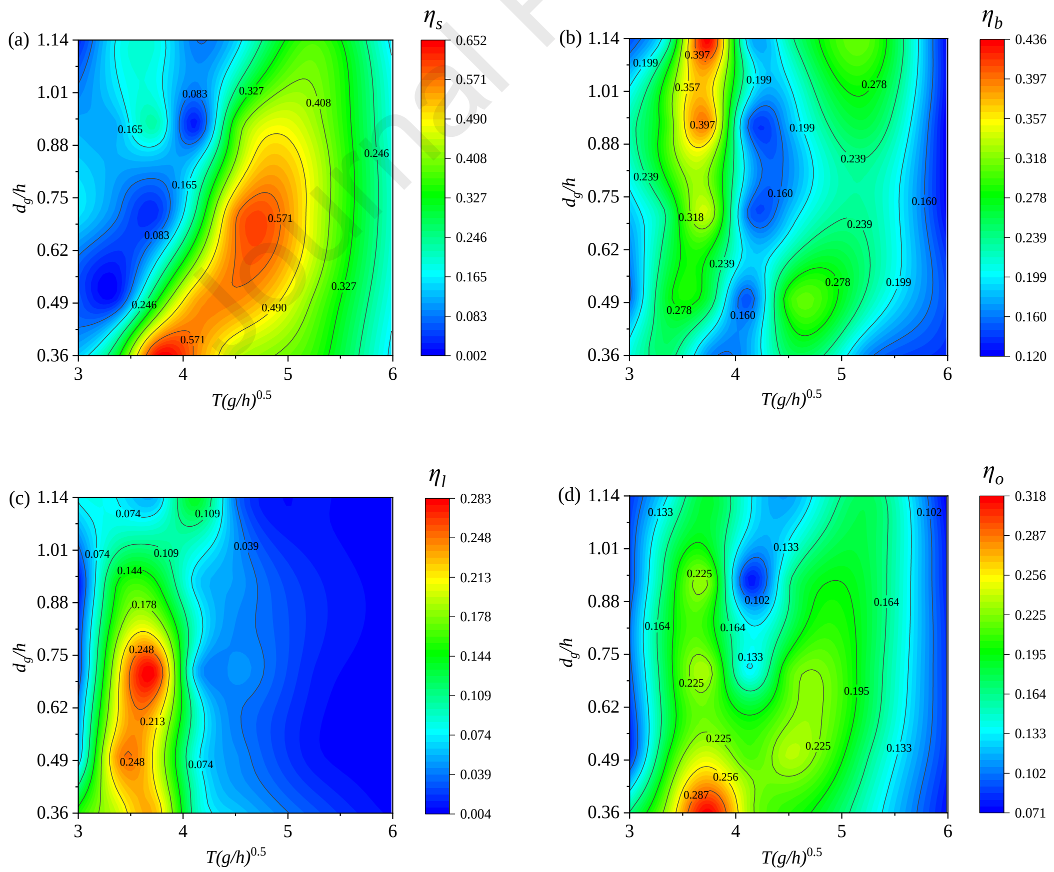

Fig. 8. Capture factor versus nondimensional wave period for different gap distance d_g/h.

(a) WEC1 (b) WEC2 (c) WEC3 and WEC4 (d) Overall hybrid system

4.3 Submerged depth effects of WECs

WEC draft is an important metric to affect the shielding effect among array WECs and the relative multi-mode motions. In this subsection, three simulation scenarios with WEC drafts d_2/h = 0.18, 0.21 and 0.25 are performed. **Fig. 9** presents the effects of WECs on the capture factor.

As plotted in **Fig. 9** (a), the efficiency peaks of the seaward WEC decrease and shift toward lower wave periods with increasing WEC draft, which is not surprising since a larger d_2/h means a larger volume of displacement occupied by the WEC, leading to a smaller natural period. What's more, the maximum capture factor of η_s can retain as higher as 0.73, extending the theoretical limit 0.5 of an isolated WEC with single rigid mode. For the leeward WEC, as presented in **Fig. 9** (b), there is a wave blocking area at wave period $T(g/h)^{0.5}$=4.1, which is independent of d_2/h. When $T(g/h)^{0.5}$ is smaller than 4.1, the capture factor decreases with increasing d_2/h, owing to short-period wave energy mainly distributed near water surface. However, when wave periods break barrier of wave-blocking period i.e. $T(g/h)^{0.5}$>4.1, the capture factor first increases and then decreases, indicating a relatively more complex multi-body and multi-mode effects. The envelope curve of η_b merges into a 'M' shaped zone. As be expected in **Fig. 9** (c), the deep submergence plays a destructive role in the energy conversion of the lateral WEC in short-period waves where the majority of surface waves is reflected toward the heading wave direction. Nevertheless, heavier water column is encased between array WECs with increasing d_2/h, which enables more energy to be dissipated from the pumping motion of water. This explains the variation of the overall efficiency with d_2/h as displayed in **Fig. 9** (d). In order to weaken the wave-energy dissipation from the near-trapping wave region and adequately convert wave energy into the multi-mode relative motion within rather wider periods, the WEC design should be as compact as possible. Indeed, the realistic heaving/pitching WEC can be devised as a flat device which can continuously extract the kinetic energy of water particles in waves and attenuate wave height at the leeward area of WECs.

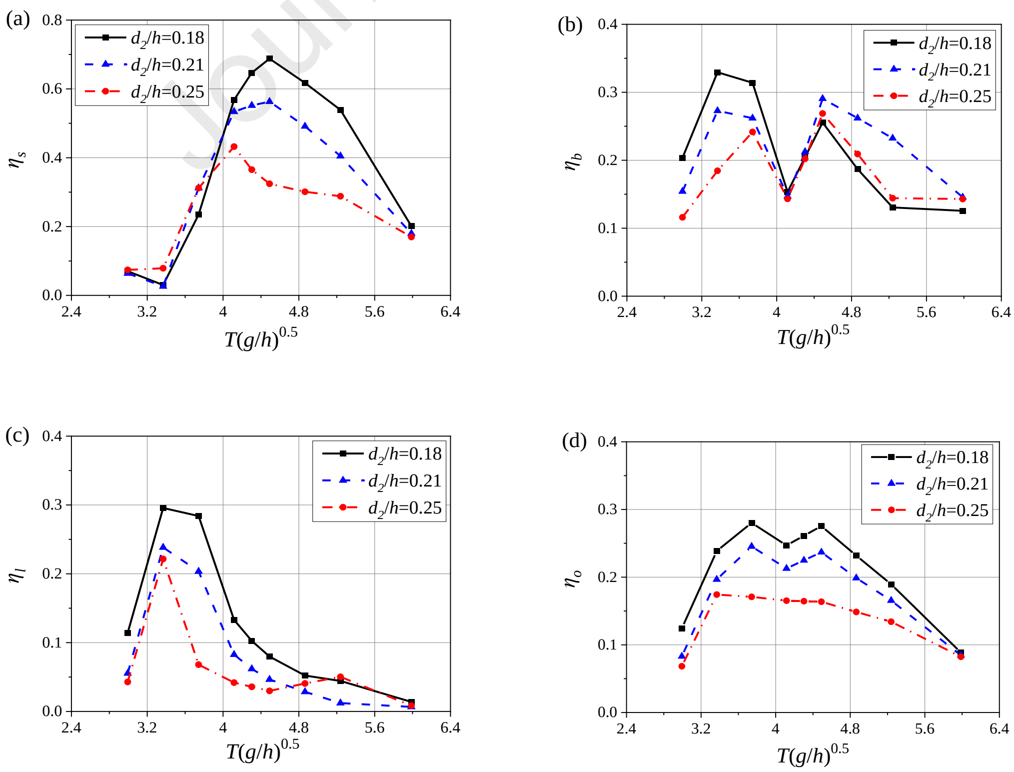

Fig. 9. Capture factor versus nondimensional wave period for different WEC draft d_2/h.

(a) WEC1 (b) WEC2 (c) WEC3 and WEC4 (d) Overall hybrid system

4.4 Optimization of the discrete PTO units

As illustrated in Eq. (15), wave energy conversion of WECs is apparently affected by the damping parameters of PTO units. All PTO units are defined to possess the same damping coefficient whose sensitivity investigations are attempted in this subsection. The geometric parameters of WECs and platform are kept the constant with Table 1 in Section 3.1. **Fig. 10** presents the efficiency contour of the overall system and respective devices as function of both wave period and PTO damping.

The optimized PTO damping varies for each WEC depending on their locations relative to the central platform. More specifically, the efficiency peak and the optimized PTO damping, are (η_s, b_{pto})=(0.63, 3.5Nms/rad), (η_b, b_{pto})=(0.33, 3.5Nms/rad or 4.9Nms/rad or 6.4Nms/rad), (η_l, b_{pto})=(0.31, 4.9Nms/rad) for the seaward WEC, the leeward WEC and the lateral WEC, respectively. Within the simulated periods and damping, the seaward and leeward WECs perform outperform the lateral WEC in terms of efficiency as well as bandwidth. Note for these WECs with optimized PTO damping, the high wave conversion performance corresponds different period ranges, suggesting that the overall performance of the hybrid system can be broadened, which is preferred for broadband irregular waves in realistic environment. Despite the PTO unit adheres to a specific mode motion to harvest wave energy, the capture factor may be larger than the acquirable capture factor in this mode, since multi-body and multi-mode interferences augment wave reflection in the array configuration.

As presented in **Fig. 10** (d), for the WEC-platform hybrid system, if identical PTO damping is adopted for all WECs, the optimal damping coefficient is b_{pto}=4.2 Nms/rad where the maximum capture factor can reach 0.26. As a comparison, no-uniform PTO damping coefficients are selected for these WECs. That's to say, every WEC is restricted with respective optimized PTO damping coefficients, i.e. b_{pto}=3.5 Nms/rad, 3.9 Nms/rad and 4.9 Nms/rad for the seaward, leeward and lateral WECs, respectively. **Fig. 11** shows the comparison of capture factor for uniform and no-uniform optimized PTO damping. It can be learned that the array WECs provide a better energy extraction performance near resonant periods i.e. $3.7<T(g/h)^{0.5}<5.2$ for the no-uniform PTO but less sensitive to the bandwidth range compared with the uniform PTO damping.

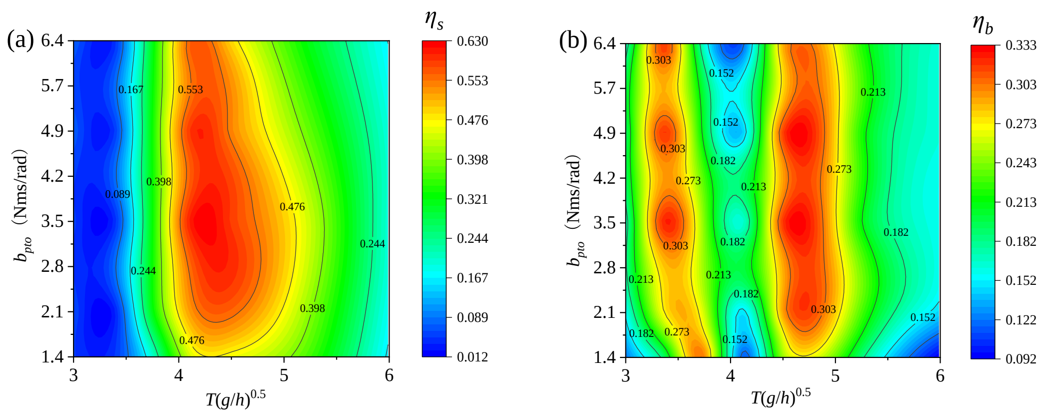

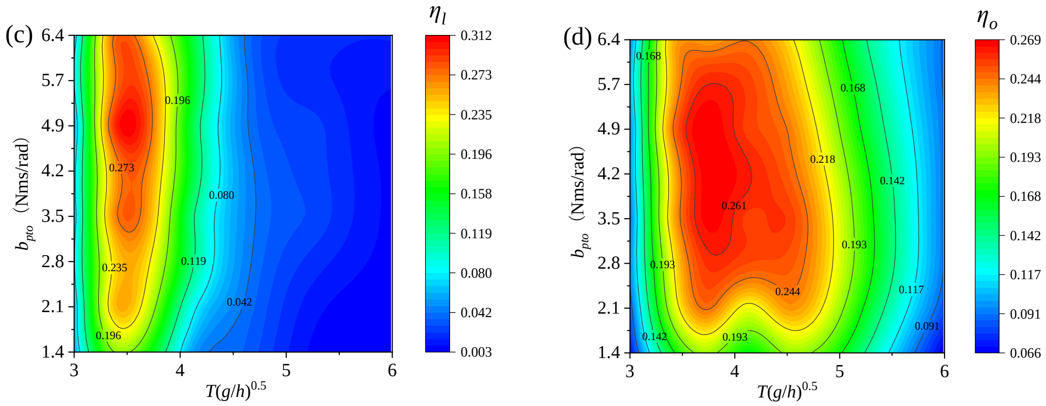

Fig. 10. Capture factor versus nondimensional wave period for different PTO damping coefficients.
(a) WEC1 (b) WEC2 (c) WEC3 and WEC4 (d) Overall hybrid system

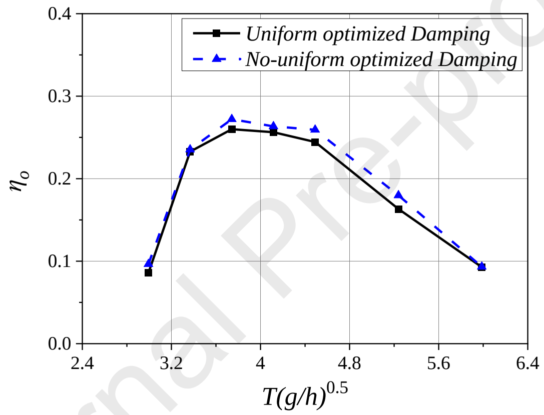

Fig. 11. The comparison of overall capture factor for uniform and no-uniform optimized PTO damping coefficients.

4.5 Dependence on incident wave direction

The simulations in the previous scenarios all contrapose the heading wave cases i.e. incident angle $\alpha = 0^o$ as shown in **Fig. 12**. Since waves is random in subsistent circumstances, different incident directions are discussed in this subsection. Array WECs of *N*=4 numbered in **Fig. 12** are uniformly deployed outward the central cylindrical platform, and thus the range of incident angles is selected over 0° to 45° according to the mirror principle of symmetry lines. **Fig. 12** presents the capture factor contour of every WEC and the overall system.

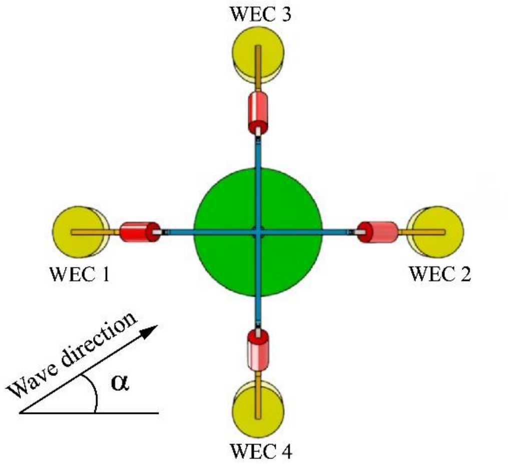

Fig. 12. Different wave directions and the hybrid system.

For any fixed period, there exists an α which provides the optimized wave absorption for all WECs, and the optimized direction of waves is sensitive to wave period which is inconsistent with the results of an isolated axisymmetric WEC. This is attributed to the gap between WECs and the platform, i.e. the gap would lead to constructive or destructive effect on the power generation depending on the gap to wavelength ratio. Except the backward WEC2 which is found to obtain two maximum capture factors for $\alpha = 0^o$, there are merely one maximum capture factor for other WECs regardless of α. The maximum capture factor for WEC1 to WEC4 are 0.55, 0.33, 0.31 and 0.75, occurring at (α, $T(g/h)^{0.5}$) = (0°, 4.5), (45°, 4.5), (9°, 3.8) and (23°, 4.7), respectively. Generally, the facing-wave WECs i.e. WEC1 and WEC4 outperform the backing-wave WECs i.e. WEC2 and WEC3. This demonstrates that the platform can direct wave energy toward facing-wave WEC in a concentrating manner, generating constructive interference, where the significant diminution for the leeward WECs is caused by the shielding effect of platform.

It is learned from **Fig. 13** (e) that as α increases from 0° to 27°, the overall maximum capture factor of the hybrid system first diminishes and shifts towards higher wave period, and then rises and shifts rapidly toward the same period in accordance with the peak capture factor of WEC4. Increasing further α, on the contrary, leads to the reduction of peak capture factor corresponding to lower wave period, which is basically dominated by the leeward WEC2. Note that, the WEC-platform configuration heading to incident waves i.e. $\alpha = 0^o$ is most effective in terms of the maximum overall energy conversion in addition to harvesting bandwidth. What's more, an additional maximum capture factor of η_o for $\alpha = 0^o$ can be excited, which is related to the WEC1 performance. This appears to indicate that within all simulated periods, there is a general identity of the maximum overall capture factor for $\alpha = 0^o$ that the WEC-platform hybrid system should observe.

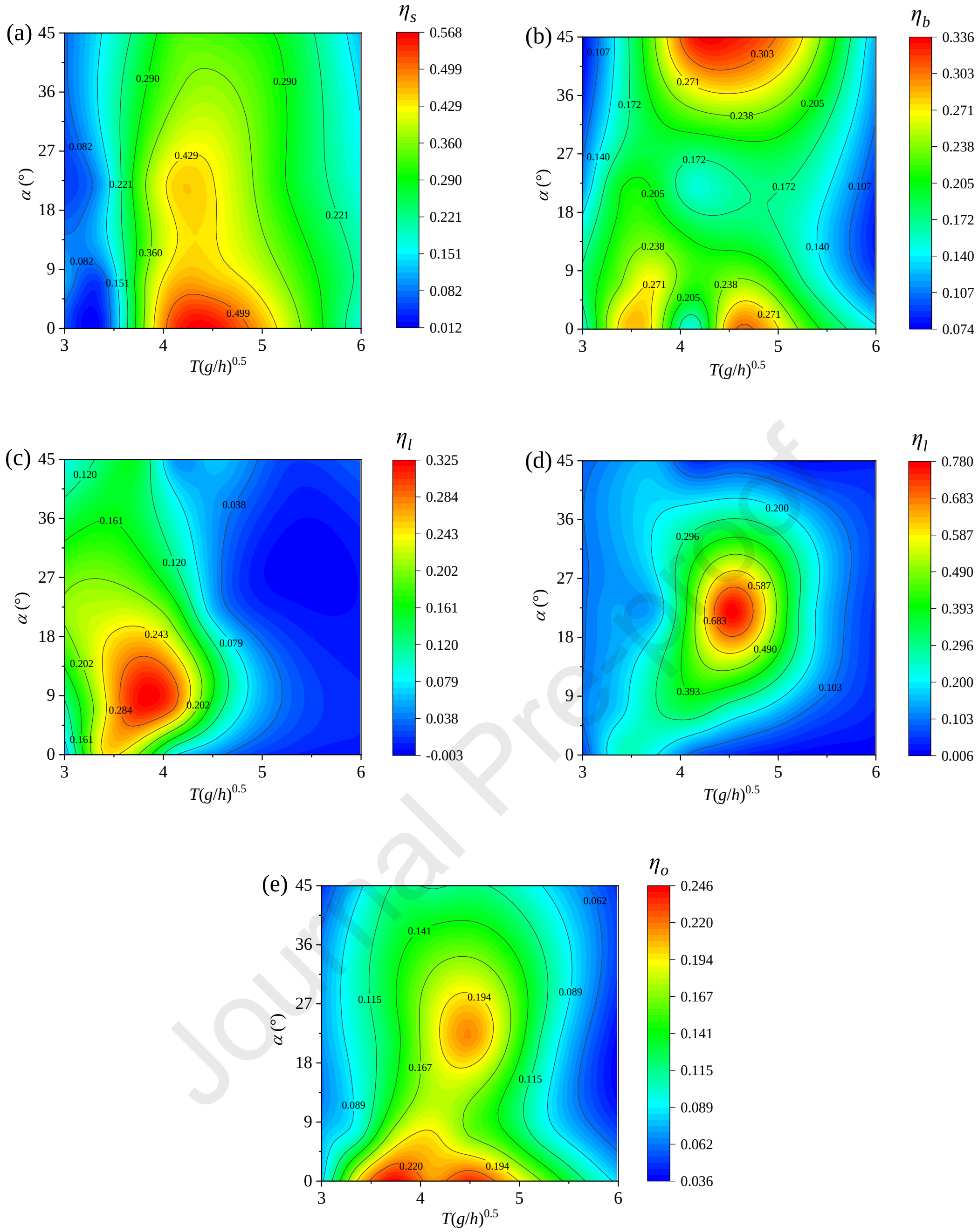

Fig. 13. Capture factor versus nondimensional wave period for different wave directions.
(a) WEC1 (b) WEC2 (c) WEC3 (d) WEC4 (e) Overall hybrid system

5 Conclusions

A hybrid system of an array of point-absorber WECs uniformly distributed around a free-floating central platform is proposed in this study. An inverted 'L' shape beam from every WEC is hinged to a 'L' shape beam that is rigidly fixed above the platform. A PTO unit is installed between the two beams to harvest wave energy from the WEC-platform relative motion of multiple modes i.e. heave, pitch and roll. Such a system, combing multi-gap resonance between adjacent floaters and multi-body resonances referring to WECs and platform, from which wave energy is extracted constructively, has not been studied before. To demonstrate the high capture factor across broadband periods, an unabridged hydrodynamic model is established based on the Computational Fluid

Dynamics (CFD)-based algorithm, where we add a moment M_{PTO} to the center of mass of the rigid body to be equivalent to the damping of the rigid body in motion. After a series of systematic simulations, the main conclusions are as follows.

(1) A hybrid system consists of a cylindrical platform and an array of cylindrical WECs are proposed. The resulting multi-body interference can be constructive or destructive depending on the spacing. More specifically, multiple reflection in the array converges wave energy, resulting a greatly enhanced relative motions of WECs and platform. However, at certain periods, a train of near-trapping waves are generated to strengthen water oscillation within local vicinity of cylinders and led to lower energy conversion.

(2) The wave energy conversion of individual WECs in the hybrid system can be balanced and the overall capture factor can substantially cover a broad period range providing an appropriate spacing between the platform and WECs. For example, short-period, moderate and long-period waves are mainly absorbed by the lateral, seaward and leeward WECs, respectively.

(3) The WEC draft provides resonance over prominent wave periods and the larger submerged depth of the platform enables multi-body resonance occurring at somewhat long wave periods, which induces two-peak capture factor of the hybrid system.

(4) Reducing WEC-platform or WEC-WEC gap distances can broaden the effective bandwidth for the seaward WEC, but has less impact on the leeward and lateral WECs. The sudden drop in the total of capture factor is induced by near-trapping waves, and shifts toward longer periods as gap distance increases. Generally speaking, a smaller gap distance is more beneficial to the overall wave energy conversion.

(5) Shallow draft of WECs cannot reduce the incidence of near-trapping waves being identified in gap, but can augment the maximum conversion efficiency as well as broadening the harvesting period range.

(6) Considering the layout of individual WECs in which the reflected, transmitted, diffracted and radiated waves by the platform play different roles, the discrete PTO system consists of different optimized PTO damping coefficients for every WEC. The results demonstrate that the optimized PTO damping coefficient increases in the order from the seaward, leeward to lateral WECs.

(7) Compared with cases of oblique waves, the higher capture factor is associated with incident waves supposed to propagate heading toward the WEC-platform hybrid system.

The WEC-Platform hybrid system would be anchored in an offshore area using multiple mooring chains which have a strong effect on the low-frequency drifting motion of floating bodies. The present CFD model is developed within the context of ignoring mooring tensions. Hence, in future study, the interaction of multi-chain hydrodynamics will be registered as a continuation of this paper.

CRediT authorship contribution statement

Yong Cheng: Methodology, Software, Data curation, Writing-original draft, Supervision. **Weifeng Liu:** Validation, Formal analysis, Writing-original draft, Investigation. **Saishuai Dai:** Formal analysis, Data curation, Writing-review & editing, Supervision. **Zhiming Yuan:** Writing-review & editing. **Atilla Incecik:** Supervision.

Declaration of Competing Interest

The authors declare that they have no known competing financial interests or personal relationships that could have appeared to influence the work reported in this paper.

Acknowledgment

The authors are grateful to the National Natural Science Foundation of China (Grant No. 52271278, 52111530137), Natural Science Found of Jiangsu province (Grant No. BK20221389) and the Newton Advanced Fellowships (Grant No. NAF\R1\180304) by the Royal Society for supporting this work.

Reference

[1] Shi XL, Liang BC, Du ST, Shao ZX, Li SW. Wave energy assessment in the China East Adjacent Seas based on a 25-year wave-current interaction numerical simulation. Renew Energy. 2022;199:1381-407.

[2] Shi XL, Li SW, Liang BC, Zhao JC, Liu Y, Wang ZL. Numerical study on the impact of wave-current interaction on wave energy resource assessments in Zhoushan sea area, China. Renew Energy. 2023;215:24.

[3] López I, Andreu J, Ceballos S, de Alegría IM, Kortabarria I. Review of wave energy technologies and the necessary power-equipment. Renew Sust Energ Rev. 2013;27:413-34.

[4] Henfridsson U, Neimane V, Strand K, Kapper R, Bernhoff H, Danielsson O, et al. Wave energy potential in the Baltic Sea and the Danish part of the North Sea, with reflections on the Skagerrak. Renew Energy. 2007;32(12):2069-84.

[5] Cheng Y, Xi C, Dai SS, Ji CY, Cocard M, Yuan ZM, et al. Performance characteristics and parametric analysis of a novel multi-purpose platform combining a moonpool-type floating breakwater and an array of wave energy converters. Appl Energy. 2021;292:18.

[6] Cheng Y, Xi C, Dai SS, Ji CY, Collu M, Li MX, et al. Wave energy extraction and hydroelastic response reduction of modular floating breakwaters as array wave energy converters integrated into a very large floating structure. Appl Energy. 2022;306:20.

[7] Zhao X, Zhou J, Wang Z, Zou Q, Renzi E. Hydrodynamic performance of multi-chamber oscillating water columns in a caisson array. Energy. 2024;305:132217.

[8] Mustapa MA, Yaakob OB, Ahmed YM, Rheem CK, Koh KK, Adnan FA. Wave energy device and breakwater integration: A review. Renew Sust Energ Rev. 2017;77:43-58.

[9] Gunn K, Stock-Williams C. Quantifying the global wave power resource. Renew Energy. 2012;44:296-304.

[10] Zhao XL, Xue FJ, Chen LH, Goteman M, Han DF, Geng J, et al. Hydrodynamic analysis of a floating platform coupled with an array of oscillating bodies. Ocean Eng. 2023;287:17.

[11] Yu D, Wang KY, Liu HX, Kong FK, Yang C, Duan YP, et al. Investigation on motion characteristics of an Anti-pitching Generating WEC (AGWEC) considering the viscous effect. Ocean Eng. 2022;246:17.

[12] Zhang HC, Xu DL, Ding R, Zhao H, Lu Y, Wu YS. Embedded Power Take-Off in hinged modularized floating platform for wave energy harvesting and pitch motion suppression. Renew Energy. 2019;138:1176-88.

[13] Zhang HC, Xu DL, Zhao H, Xia SY, Wu YS. Energy extraction of wave energy converters embedded in a very large modularized floating platform. Energy. 2018;158:317-29.

[14] Nguyen HP, Wang CM, Flocard F, Pedroso DM. Extracting energy while reducing hydroelastic responses of VLFS using a modular raft wec-type attachment. Appl Ocean Res. 2019;84:302-16.

[15] Nguyen HP, Wang CM. Oscillating Wave Surge Converter-Type Attachment for Extracting Wave Energy While Reducing Hydroelastic Responses of Very Large Floating Structures. J Offshore Mech Arct Eng Trans ASME. 2020;142(4):9.

[16] Nguyen HP, Wang CM, Tay ZY, Luong VH. Wave energy converter and large floating platform integration: A review. Ocean Eng. 2020;213:17.

[17] Zhang HC, Xu DL, Liu CR, Wu YS. Wave energy absorption of a wave farm with an array of buoys and flexible runway. Energy. 2016;109:211-23.

[18] Zhou BZ, Hu JJ, Jin P, Sun K, Li Y, Ning DZ. Power performance and motion response of a floating wind platform and multiple heaving wave energy converters hybrid system. Energy. 2023;265:12.

[19] Liao ZJ, Stansby P, Li G. A generic linear non-causal optimal control framework integrated with wave excitation force prediction for multi-mode wave energy converters with application to M4. Appl Ocean Res. 2020;97:8.

[20] Ma Y, Xie GC, Liu S, Zhao TC, Zhu YY, Zhang X. Hydrodynamic performance investigation of the multi-degree of freedom oscillating-buoy wave energy converter. Ocean Eng. 2023;285:10.

[21] Stansby P, Moreno EC, Stallard T, Maggi A. Three-float broad-band resonant line absorber with surge for wave energy conversion. Renew Energy. 2015;78:132-40.

[22] Stansby P, Moreno EC, Stallard T. Large capacity multi-float configurations for the wave energy converter M4 using a time-domain linear diffraction model. Appl Ocean Res. 2017;68:53-64.

[23] Lande-Sudall DR, Nyland J, Rykkje TR, Stansby PK, Impelluso T. Hydrodynamic modelling of a multi-body wave energy converter using the Moving Frame Method. Mar Struct. 2023;87:17.

[24] Tran N, Sergiienko NY, Cazzolato BS, Ding B, Wuillaume PY, Ghayesh MH, et al. On the importance of nonlinear hydrodynamics and resonance frequencies on power production in multi-mode WECs. Appl Ocean Res. 2021;117:14.

[25] Zeng XH, Wang Q, Kang YS, Yu FJ. A Novel Type of Wave Energy Converter with Five Degrees of Freedom and Preliminary Investigations on Power-Generating Capacity. Energies. 2022;15(9):20.

[26] Kara F. Time domain prediction of power absorption from ocean waves with wave energy converter arrays. Renew Energy. 2016;92:30-46.

[27] Yazdi H, Ghafari HR, Ghassemi H, He GH, Karimirad M. Wave power extraction by Multi-Salter's duck WECs arrayed on the floating offshore wind turbine platform. Energy. 2023;278:17.

[28] He GH, Luan ZX, Jin RJ, Zhang W, Wang W, Zhang ZG, et al. Numerical and experimental study on absorber-type wave energy converters concentrically arranged on an octagonal platform. Renew Energy. 2022;188:504-23.

[29] He G, Liu C, Zhang W, Luan Z, Zhang Z. Numerical study of the effect of central platform motion on the wave energy converter array. Ocean Eng. 2023;286:115483.

[30] Kamarlouei M, Gaspar JF, Calvario M, Hallak TS, Mendes M, Thiebaut F, et al. Experimental study of wave energy converter arrays adapted to a semi-submersible wind platform. Renew Energy. 2022;188:145-63.

[31] Kamarlouei M, Gaspar JF, Calvario M, Hallak TS, Mendes M, Thiebaut F, et al. Experimental analysis of wave energy converters concentrically attached on a floating offshore platform. Renew Energy. 2020;152:1171-85.

[32] Jin SY, Wang DM, Hann M, Collins K, Conley D, Greaves D. A designed two-body hinged raft wave energy converter: From experimental study to annual power prediction for the EMEC site using WEC-Sim. Ocean Eng. 2023;267:16.

[33] Bai W, Feng X, Taylor RE, Ang KK. Fully nonlinear analysis of near-trapping phenomenon around an array of cylinders. Appl Ocean Res. 2014;44:71-81.

[34] Cheng Y, Song F, Dai S, Yuan Z, Incecik A. Broadband wave energy extraction by a dual-PTO hybrid system of a comb-type breakwater and an oscillating flap. Energy Conversion and

Management. 2023;297:117670.

Highlights:

1. Multi-mode exciting WECs are arrayed around a free-floating platform.
2. The wave focusing toward WECs is realized by the array reflection.
3. The presence of near-trapping waves in the array amplifies energy dissipation.
4. The narrower array interval leads to the higher overall conversion efficiency.
5. The hybrid system can harvest wave energy in an omnidirectional manner.

Declaration of interests

☒ The authors declare that they have no known competing financial interests or personal relationships that could have appeared to influence the work reported in this paper.

☐ The authors declare the following financial interests/personal relationships which may be considered as potential competing interests: